

Revealing anyonic statistics with multiphoton entanglement

J. K. Pachos¹, W. Wieczorek^{2,3}, C. Schmid^{2,3}, N. Kiesel^{2,3}, R. Pohlner^{2,3} & H. Weinfurter^{2,3}

¹*School of Physics & Astronomy, University of Leeds, Leeds LS2 9JT, UK*

²*Max-Planck-Institute of Quantum Optics, D-85748 Garching, Germany*

³*Department for Physics, Ludwig-Maximilians-Universität München, D-80799 München, Germany*

The collective statistical behaviour of quantum particles is, according to Pauli, determined by their spin¹. In three spatial dimensions, there are only two possible types of statistics, dividing particles into two groups: bosons and fermions. However, if one is restricted to two-dimensional systems the situation changes drastically. There, anyons² can appear, which exhibit fractional statistics ranging continuously from bosonic to fermionic behaviour. This is manifested by the observation that their quantum state can acquire “any” phase when one anyon is exchanged with another one, in contrast to the restricted values $+1$ for bosons and -1 for fermions. Anyons are responsible for the fractional quantum Hall effect and should be realized as quasiparticles in highly entangled many-body systems³. The isolation of anyons in these systems requires cooling to very low temperatures where only the ground and a few excited states are populated. However, the continuing presence of interactions makes anyons quite elusive and, despite substantial experimental effort, their definitive detection remains open⁴⁻⁶. Here, as an alternative approach, we encode the relevant many-body state of an anyonic model⁷ in the multi-partite entangled state of polarized photons. This quantum system is intrinsically stable against decoherence. It enables easy manipulation and detection of abelian⁸ anyons, allows for the demonstration of their fusion rules and facilitates the unambiguous determination of their statistical properties. The experiments directly demonstrate the presence of fractional statistics in a physical system.

The concept of anyons² first emerged in connection with the fractional quantum Hall effect⁹, which appears in a two dimensional electron gas at low temperatures when it is subject to a perpendicular magnetic field. Such conditions result in a strongly correlated quantum system, where the excitations are anyonic quasiparticles with fractional charge¹⁰. Formally, the properties of anyons are described by two dimensional topological quantum field theories¹¹ that dictate their trivial dynamical, but complex statistical behaviour. In general, it is expected that topological quantum field theories come into effect at low energies of highly correlated many-body systems, such as quantum liquids¹². In these systems, anyons emerge as spatially localized many-body states that can be generated and transported by local operations. These states are highly entangled with long range coherences that allow anyons to exhibit fractional statistics. However, the observation of anyonic features requires high population in the system’s ground state, high purity samples and, above all, the ability to separate the anyonic effects from the dynamical background of the strongly interacting system. In spite of significant experimental progress the fractional statistics of anyons has not

yet been conclusively confirmed in the laboratory⁴⁻⁶.

Here we employ a different strategy by realizing anyonic states in a quantum system without any interactions at all¹³. The scheme is based on the fact that the statistical properties of anyons are manifested solely by the evolution of the wave function of the underlying system, independent of the presence of a Hamiltonian. Remarkably, as we will show in the following, four-partite entangled GHZ states¹⁴ are sufficient to reveal anyonic statistics. These states are dynamically encoded in the polarization of photons, rather than produced via cooling. Thus, they are subject to negligible decoherence and allow for the efficient manipulation and detection of anyons. Polarized photons as qubits are a well understood and controllable quantum optical system that already allowed to observe the four-qubit GHZ state¹⁵. Hence, they are ideally suited to emulate the dynamics of a system whose control would otherwise be experimentally challenging. Here we perform novel manipulation procedures and analyse their effect on the GHZ states with the aim to clearly reveal anyonic statistics. For the observation of the multi-partite entangled states we use photons generated by spontaneous parametric down conversion (SPDC) and their subsequent processing by a linear optical network. The local rotations, necessary for the manipulation of anyons, can be implemented by wave plates acting on the particular photons (see Methods). The anyonic manipulations performed here are exactly the same as required for larger systems or in the presence of a Hamiltonian.

The anyonic model under consideration is based on the toric code proposed by Kitaev⁷. It was introduced with the aim of storing and processing quantum information in a fault-tolerant way and is described in detail in tutorial introductions¹⁶. This system can be defined on a two dimensional square lattice with interacting qubits placed at its vertices. To facilitate the description of the interactions let us split the lattice into two alternating types of plaquettes labelled by p and s as in Fig. 1. The defining Hamiltonian is

$$\mathcal{H} = - \sum_p \sigma_{p,1}^z \sigma_{p,2}^z \sigma_{p,3}^z \sigma_{p,4}^z - \sum_s \sigma_{s,1}^x \sigma_{s,2}^x \sigma_{s,3}^x \sigma_{s,4}^x, \quad (1)$$

where the summations run over the corresponding plaquettes and the indices 1, ..., 4 of the Pauli operators, σ^z and σ^x , number the vertices of each plaquette in a counter-clockwise fashion. Each of the s - or p -plaquette interaction terms commute with the Hamiltonian as well as with each other. Thus, the model is exactly solvable¹⁷ and its ground state is explicitly given by

$$|\xi\rangle = \prod_s \frac{1}{\sqrt{2}} (\mathbb{1} + \sigma_{s,1}^x \sigma_{s,2}^x \sigma_{s,3}^x \sigma_{s,4}^x) |00\dots 0\rangle, \quad (2)$$

with $\sigma^z|0\rangle = |0\rangle$. The state $|\xi\rangle$ represents the anyonic vacuum state. Starting from this ground state one can excite pairs of anyons connected by a string on the lattice using single qubit operations. More specifically, by applying σ^z on some qubit of the lattice a pair of so called e -type anyons in the state $|e\rangle = \sigma^z|\xi\rangle$ is created on the two neighbouring s plaquettes (Fig. 1a). An m pair of anyons given by $|m\rangle = \sigma^x|\xi\rangle$ on the p plaquettes is obtained by a σ^x transformation. The

combination of both creates the composite quasiparticle ϵ with $|\epsilon\rangle = \sigma^z \sigma^x |\xi\rangle = i\sigma^y |\xi\rangle$. Two equal Pauli rotations applied on qubits of the same plaquette create two anyons on this plaquette. The fusion rules ($1 \times 1 = e \times e = m \times m = \epsilon \times \epsilon = 1$, $e \times m = \epsilon$, $1 \times e = e$, etc.¹⁶) describe the outcome from combining two anyons, i.e., in the above example the annihilation of anyons on the same plaquette. Thereby, two single strings of the same type can be glued together to a new string, again with a pair of anyons at its ends (Fig. 1b). If the string, or a part of it, forms a loop, the anyons at its end annihilate each other thus removing the anyonic excitation, or the string gets truncated (Fig. 1c), respectively. For an open system, such as the one we consider here, a string may end up at the boundary describing a single anyon at its free endpoint.

The anyonic character is revealed as a non-trivial phase factor acquired by the wave function of the lattice system after braiding anyons, i.e., after moving m around e (Fig. 1d) or vice versa. Consider the initial state $|\Psi_{\text{ini}}\rangle = \sigma_1^z |\xi\rangle = |e\rangle$. If an anyon of type m is assumed to be at a neighbouring p plaquette it can be moved around e along the path generated by successive applications of σ^x rotations on the four qubits of the s plaquette. The final state is

$$|\Psi_{\text{fin}}\rangle = \sigma_1^x \sigma_2^x \sigma_3^x \sigma_4^x |\Psi_{\text{ini}}\rangle = -\sigma_1^z (\sigma_1^x \sigma_2^x \sigma_3^x \sigma_4^x |\xi\rangle) = -|\Psi_{\text{ini}}\rangle. \quad (3)$$

Such a minimal loop also corresponds to the application of the respective interaction term $C_m = \sigma_{s,1}^x \sigma_{s,2}^x \sigma_{s,3}^x \sigma_{s,4}^x$ (or $C_e = \sigma_{p,1}^z \sigma_{p,2}^z \sigma_{p,3}^z \sigma_{p,4}^z$) of the Hamiltonian. This operator has eigenvalue $+1$ for all plaquettes of the ground state $|\xi\rangle$, whereas it signals an excitation, e.g., $|\Psi_{\text{ini}}\rangle$, with eigenvalue -1 , when applied to the plaquette where an anyon resides. However, equation (3) is much more general, as the actual path of the loop is irrelevant (Fig. 1e). It is the topological phase factor of -1 , which reveals the presence of the enclosed anyon. Alternatively, we can interpret equation (3) as a description of twisting ϵ , the combination of an e and an m -type anyon, by 360° (Fig. 1f). The phase factor of -1 thereby reveals its 4π -symmetry, characteristic for half spin, fermionic particles¹⁸. Note that the e (m) anyons exhibit bosonic character with respect to each other.

As this two dimensional system is well suited for demonstrating characteristic anyonic features, the question arises how big the lattice has to be. Here we consider an s plaquette¹⁹ that comprises of four qubits. The neighbouring four p plaquettes are made up from eight additional qubits (see Fig. 1a). As seen from Eqn. (2) the ground state describing the extended system separates into a four qubit GHZ state for the s plaquette ($|\xi\rangle = (|0000\rangle + |1111\rangle)/\sqrt{2}$) and a fully separable eight qubit state, which factors from this core. It will be seen in the following that this system is sufficiently large to describe most of the fusion and statistical properties of the toric code anyons. In this system an e anyon can live in the s plaquette with its string ending at the boundary of the system, while m anyons can be generated and transported in the neighbouring p plaquettes. As the additional qubits of the p plaquettes actually factor from the state of the core we will focus in the following on the four qubits of a single s plaquette without compromising the physical properties we want to demonstrate²⁰. This is a significant simplification compared to the proposal of Han *et al.*¹³ that requires six qubits for realizing the same single plaquette. In addition, here we propose and implement the corresponding fusion rules of the anyons.

In the experiment the qubits supporting the anyonic states are encoded in the polarization of single photons propagating in well-defined spatial modes. This means that for the anyonic vacuum and for all obtained final states our system is of the form $|\text{GHZ}^\phi\rangle = (|H_1H_2H_3H_4\rangle + e^{i\phi}|V_1V_2V_3V_4\rangle)/\sqrt{2}$. The indices (omitted in the following) label the spatial mode of each photon, i.e., they represent the position of the qubit as in Fig. 1d, and H(V) denote linear horizontal (vertical) polarization, representing a logical 0 (1). To obtain such four-photon entangled states, the second order emission of a non-collinear type-II SPDC, yielding four photons in two spatial modes, is overlapped on a polarizing beam splitter (PBS) and afterwards symmetrically split up into four spatial modes by two polarization independent beam splitters (see Fig. 2a). Prior to the second order interference at the PBS the polarization of two of the photons is rotated by a half-wave plate. Under the condition of detecting one photon in each spatial mode we observe the desired states. Further details on the state observation can be found in the Methods section.

As we are interested in the vacuum $|\xi\rangle = |\text{GHZ}^0\rangle$ and the anyon $|e\rangle = \sigma_i^z|\xi\rangle = |\text{GHZ}^\pi\rangle$, the successful experimental demonstration and manipulation of anyons relies on a careful distinction and characterization of these two orthogonal GHZ states. This comprises the confirmation of genuine four-partite entanglement and a method to reveal the phase ϕ . The state analysis can be performed²¹ by measuring the correlation in the $\sigma_1^z\sigma_2^z\sigma_3^z\sigma_4^z$ basis and the correlation function $c_{xy}(\gamma) = \sigma_1(\gamma) \otimes \sigma_2(\gamma) \otimes \sigma_3(\gamma) \otimes \sigma_4(\gamma)$ with $\sigma_i(\gamma) = [(\cos \gamma)\sigma_i^y + (\sin \gamma)\sigma_i^x]$ (see Fig. 2b-d and Methods).

We start the experimental demonstration by analysing the state change under the creation (and annihilation) of anyons, thereby demonstrating the characteristic fusion rules. Applying the operation σ_1^z in mode 1 creates an e -type anyon on the s plaquette resulting in a GHZ^π state (Fig. 3a). This is clearly proven by the phase of the correlation function determined by a sinusoidal fit to be $\phi = 1.02\pi$ (here and in the following, the statistical error on the phase determination is approximately 0.01π , see Supplementary Table S1). However, a further application of σ_j^z on any other mode, say $j = 3$, changes the state of the plaquette according to $e \times e = 1$, and the anyon is moved away from the considered s plaquette. These two σ^z rotations represent a string connecting two anyons, which traverses the plaquette under observation, without influencing its state, as confirmed by the observation of the GHZ^0 state ($\phi = 0.01\pi$, Fig. 3b). A further σ_j^z rotation on one of the remaining vertices, e.g., $j = 4$, creates an e occupation on the plaquette. Thus, the observation of GHZ^π ($\phi = 1.03\pi$, Fig. 3c) demonstrates the non-trivial version of the $1 \times e = e$ fusion rule. Alternatively, this can be seen as demonstrating the invariance of an anyonic state, when a string traverses the plaquette.

To detect the major feature of anyons, their non trivial statistical phase obtained by their braiding, we employed an interference measurement, which makes their *global* phase factor visible (see equation (3) and Fig. 1d). Let us first study the two evolutions separately. The first is to move an m anyon around an empty plaquette. This s plaquette loop C_m , obviously, does not change the vacuum state and thus results in GHZ^0 ($\phi = -0.02\pi$, Fig. 4a). Alternatively, we create an e on the plaquette, encompass it with the loop of an m anyon, and remove it again. The whole

evolution is, in analogy to equation (3), described by $\sigma_1^z(\sigma_1^x\sigma_2^x\sigma_3^x\sigma_4^x)\sigma_1^z|\xi\rangle = -|\xi\rangle = -|\text{GHZ}^0\rangle$. The correlation function determines faithfully the angle $\phi = -0.01\pi$ (Fig. 4b), but is blind to the characteristic global phase factor. This, finally, can be observed by first generating the *superposition* $e^{-i\pi/4}(|\xi\rangle + i|e\rangle)/\sqrt{2}$ of having an anyon e on the plaquette or not by the unitary operation $(\sigma_i^z)^{-1/2}$. Acting with the s plaquette loop C_m gives $e^{-i\pi/4}(|\xi\rangle - i|e\rangle)/\sqrt{2}$, the superposition of the above evolutions. The application of the inverse rotation $(\sigma_i^z)^{1/2}$ makes the phase difference visible resulting in $-i|e\rangle = -i|\text{GHZ}^\pi\rangle$, compared to the GHZ^0 state without a global phase difference. Note that, if the Hamiltonian (1) were present during the interference procedure, a dynamical phase factor would have easily dephased the superposition between the anyonic vacuum, $|\xi\rangle$, and the anyonic state, $|e\rangle$, making the detection of the statistical angle significantly harder. The observed value of $\phi = 1.00\pi$ (Fig. 4c) clearly proves the phase acquired by the braiding and therefore the fractional statistics of anyons.

These results show that we can create, manipulate and detect anyonic states, demonstrate their fusion rules and determine their fractional statistics on a simple physical system. This satisfies a broad interest in physically realizing these exotic particles^{22,23}. On a larger scale this gives the opportunity to harness them for potential future applications, e.g., the toric code states are codewords for performing quantum error correction, a property that makes their physical realization an ideal venue for quantum information storing and processing²⁴. While the absence of a Hamiltonian in our scheme does not affect its topological and error correcting properties, fault tolerant quantum computation would require the presence of a Hamiltonian²⁵. In a sense our four-photon set-up is an elementary quantum simulator for a simple topological theory. The measurements described here are the first single qubit manipulations on a mighty encoding scheme. The extension of our results to larger, scalable systems²⁶ as well as their alternative implementation, e.g., with ultra cold molecules²⁷, can lead to a better understanding of the control and application of anyons.

Methods

State observation. Figure 2a displays the experimental set-up for the observation of the anyonic vacuum state of the toric code model and the verification of anyonic statistics. As photon source we use type II, non-collinear spontaneous parametric down conversion²⁸ (SPDC). A 2mm thick β Barium Borate (BBO) crystal is pumped by femtosecond UV pulses having an average power of approximately 700 mW and a central wavelength of 390 nm. The UV pulses are obtained from a frequency doubled mode-locked Ti:Sapphire laser. The down converted photons are coupled into single mode fibres exactly defining the spatial modes a and b . Transversal and longitudinal walk-off effects due to birefringence in the BBO crystal are compensated for by a half-wave plate (HWP) and a 1 mm thick BBO crystal in each spatial mode prior to the coupling. Spectral selection is achieved by interference filters (not shown) with a full width at half maximum of 3 nm centred around the degenerate wavelength of 780 nm. The source is aligned such that the first order SPDC emission yields entangled pairs in the Bell state $|\psi^+\rangle_{ab} = (|H\rangle_a|V\rangle_b + |V\rangle_a|H\rangle_b)/\sqrt{2}$ at a mean visibility of 98% in the H/V basis and 93% in the $+/-$ basis (with $|\pm\rangle = (|H\rangle \pm |V\rangle)/\sqrt{2}$). For

the observation of the anyonic states, we are interested in the second order emission of SPDC that provides four photons²⁹ initially emitted in the two spatial modes a and b . These photons are in the state $\propto |2H\rangle_a|2V\rangle_b + |2V\rangle_a|2H\rangle_b + |HV\rangle_a|HV\rangle_b$ which is further processed by linear optical elements: In spatial mode b a HWP is inserted before both modes are overlapped on a polarization-dependent beam splitter (PBS) that transmits (reflects) horizontally (vertically) polarized photons. The HWP transforms $|H\rangle$ into $|+\rangle$ and $|V\rangle$ into $|-\rangle$. The photons at the outputs a' and b' of the PBS are distributed by polarization-independent beam splitters (BS) onto four spatial modes. (Not shown are birefringent optical elements compensating for an unwanted phase introduced by each beam splitter.) The state $|\xi\rangle$ is observed under the condition of detecting a photon in each of the four modes. We find an average fourfold count rate of 2.8 min^{-1} . The local operations (LO) for the verification of anyonic statistics are implemented by operation specific HWPs and quarter-wave plates (QWP) as indicated in Fig. 2a. The polarization state of each photon is analysed (PA) with a HWP and a QWP in front of a PBS in order to perform the necessary correlation measurements of all photons. Finally, the photons are detected by Silicon-avalanche photo diodes.

State characterization. The observation of the state $|\xi\rangle = |\text{GHZ}^0\rangle$ has to be confirmed. We start with a correlation measurement in the basis $\sigma_1^z\sigma_2^z\sigma_3^z\sigma_4^z$ (Fig. 2b). Figure 2c shows all possible measurement outcomes in this basis where the expected populations of $|\text{HHHH}\rangle$ and $|\text{VVVV}\rangle$ are clearly predominant with probabilities of $P_{\text{HHHH}} = (41.2 \pm 3.4)\%$ and $P_{\text{VVVV}} = (39.6 \pm 2.7)\%$, respectively, close to the expected $P_{\text{HHHH}} = P_{\text{VVVV}} = 50\%$. The population of other terms is caused by noise arising from higher-order emissions of the down conversion and a remaining degree of distinguishability of independent photons at the overlap beam splitter. To prove that the terms $|\text{HHHH}\rangle$ and $|\text{VVVV}\rangle$ are in a coherent superposition and to determine their relative phase ϕ we chose to measure the correlation function $c_{xy}(\gamma) = \sigma_1(\gamma) \otimes \sigma_2(\gamma) \otimes \sigma_3(\gamma) \otimes \sigma_4(\gamma)$ with $\sigma_i(\gamma) = [(\cos \gamma)\sigma_i^y + (\sin \gamma)\sigma_i^x]$ (see Fig. 2d). It is obtained from a simultaneous measurement of each qubit along the x - y plane of the Bloch sphere (see Fig. 2b) and therefore corresponds to a joint measurement on all qubits²¹, capable of examining global state properties. Its expectation value for a GHZ^ϕ state is supposed to show an oscillation, $\langle c_{xy}(\gamma) \rangle = \mathcal{V} \cos(4\gamma + \phi)$, with a period of one quarter of 2π which is a unique signature of four qubit GHZ entanglement. The visibility \mathcal{V} is 1 for pure GHZ states. For a general state it equals twice the element $\rho_{\text{HHHH},\text{VVVV}} = \text{Tr}[|\text{HHHH}\rangle\langle\text{VVVV}|\rho]$ of the corresponding density matrix ρ and is thus a measure of coherence between the typical GHZ terms. The measured correlation function for the anyonic vacuum state is displayed in Fig. 2d from which we infer a visibility \mathcal{V} of $(68.3 \pm 1.1)\%$. From the phase of the correlation $\langle c_{xy}(\gamma) \rangle$ we deduce the phase of the GHZ^0 state to be $\phi = (0.02 \pm 0.01)\pi$ close to the expected value of 0. The visibility of the correlation function together with the populations P_{HHHH} and P_{VVVV} allow further to determine the fidelity $F = \langle \text{GHZ}|\rho|\text{GHZ} \rangle = (\mathcal{V} + P_{\text{HHHH}} + P_{\text{VVVV}})/2$. We obtain a value of $(74.5 \pm 2.2)\%$ (all data shown here are from measurements with at least this fidelity, see Supplementary Table S1). The fidelity is not only important for an estimation of state quality but can also be applied to verify genuine four-partite entanglement – an essential element in the presented toric code model. A fidelity greater than 50% is sufficient³⁰ once a proper entanglement witness is used. The experimentally observed fidelity is clearly above this bound, so we can employ our set-up to demonstrate the anyonic properties predicted by the toric code.

1. Pauli, W., The Connection Between Spin and Statistics, *Phys. Rev.* **58**, 716-722 (1940).
2. Wilczek, F., Magnetic Flux, Angular Momentum, and Statistics, *Phys. Rev. Lett.* **48**, 1144-1146 (1982).
3. Laughlin, R. B., Anomalous Quantum Hall Effect: An Incompressible Quantum Fluid with Fractionally Charged Excitations, *Phys. Rev. Lett.* **50**, 1395-1398 (1983).
4. Camino, F. E., Zhou, W. & Goldman, V. J., $e/3$ Laughlin Quasiparticle Primary-Filling $\nu = 1/3$ Interferometer, *Phys. Rev. Lett.* **98**, 076805 (2007).
5. Camino, F. E., Zhou, W. & Goldman, V. J., Aharonov-Bohm Superperiod in a Laughlin Quasiparticle Interferometer, *Phys. Rev. Lett.* **95**, 246802 (2005).
6. Rosenow, B. & Halperin, B. I., Influence of Interactions on Flux and Back-Gate Period of Quantum Hall Interferometers, *Phys. Rev. Lett.* **98**, 106801 (2007).
7. Kitaev, A., Fault-tolerant quantum computation by anyons, *Ann. Phys. (N.Y.)* **303**, 2-30 (2003).
8. Abelian anyons exhibit a statistics that corresponds to a complex phase factor when two anyons are braided, i.e. one anyon is moved around the other. In the non-abelian case a general unitary can be obtained. In the following, whenever we talk about anyons, we tacitly refer to the abelian ones.
9. Tsui, D. C., Stormer, H. L. & Gossard, A. C., Two-Dimensional Magnetotransport in the Extreme Quantum Limit, *Phys. Rev. Lett.* **48**, 1559-1562 (1982).
10. de-Picciotto *et al.*, Direct observation of a fractional charge, *Nature* **389**, 162-164 (1997).
11. Witten, E., Quantum field theory and the Jones polynomial, *Commun. Math. Phys.* **121**, 351-399 (1989).
12. Anderson, P. W., The resonating valence bond state in La₂CuO₄ and superconductivity, *Science* **235**, 1196 (1987).
13. Han Y.-J., Raussendorf, R., & Duan, L.-M., Scheme for Demonstration of Fractional Statistics of Anyons in an Exactly Solvable Model, *Phys. Rev. Lett.* **98**, 150404 (2007).
14. Greenberger, D. M., Horne, M. A. & Zeilinger, A. in *Bell's Theorem, Quantum Theory, and Conceptions of the Universe* (ed. Kafatos, M.) 73-76 (Kluwer Academic, Dordrecht, 1989).
15. Pan, J.W., Daniell, M., Gasparoni, S., Weihs, G. and Zeilinger, A., Experimental Demonstration of Four-Photon Entanglement and High-Fidelity Teleportation, *Phys. Rev. Lett.* **86**, 4435 (2001).
16. Preskill, J., Lecture Notes for Physics 219: Quantum Computation, <http://www.theory.caltech.edu/~preskill/>.

17. Verstraete, F. *et al.*, Criticality, the Area Law, and the Computational Power of Projected Entangled Pair States, *Phys. Rev. Lett.* **96**, 220601 (2006).
18. Rauch, H. *et al.*, Verification of coherent spinor rotation of fermions, *Phys. Lett. A* **54**, 425-427 (1975).
19. Pachos, J. K., The Wavefunction of an Anyon, *Ann. Phys.* **322**, 1254-1264 (2007).
20. We have experimentally performed the manipulations of the extra qubits of the p plaquettes on additional four-photon events and observed fidelities $> 98\%$.
21. Sackett, C. A. *et al.*, Experimental entanglement of four particles, *Nature* **404**, 256-259 (2000).
22. Das Sarma, S., Freedman, M., & Nayak, C., Topological protected qubits from a possible non-Abelian fractional quantum Hall state, *Phys. Rev. Lett.* **94**, 166802 (2005).
23. Bonderson, P., Shtengel, K., & Slingerland, J. K., Probing Non-Abelian Statistics with Quasi-particle Interferometry, *Phys. Rev. Lett.* **97**, 016401 (2006).
24. Kitaev, A., Quantum computation: algorithms and error correction, *Russian Math. Surveys*, 52 (6) (1997) 1191.
25. Freedman, M. H., Kitaev, A., Larsen, M. J. & Wang, Z., Topological quantum computation, *Bull. Amer. Math. Soc.* **40**, 31-38 (2003).
26. Raussendorf, R., Bravyi, S., & Harrington, J., Long-range quantum entanglement in noisy cluster states, *Phys. Rev. A* **71**, 062313 (2005).
27. Micheli, A., Brennen, G. K., & Zoller, P., A toolbox for lattice spin models with polar molecules, *Nature Physics* **2**, 341-347 (2006).
28. Kwiat, P. G., Mattle, K., Weinfurter, H. & Zeilinger, A., New High-Intensity Source of Polarization-Entangled Photon Pairs, *Phys. Rev. Lett.* **75**, 4337-4341 (1995).
29. Eibl, M. *et al.*, Experimental observation of Four-photon entanglement from parametric down-conversion, *Phys. Rev. Lett.* **90**, 200403 (2003).
30. Toth, G. & Gühne, O., Detecting Genuine Multipartite Entanglement with Two Local Measurements, *Phys. Rev. Lett.* **94**, 060501 (2005).

Acknowledgements J.K.P. would like to thank Phillippe Grangier for inspiring conversations. We acknowledge the support of this work by Deutsche Forschungsgemeinschaft through the DFG-Cluster of Excellence “Munich Centre for Advanced Photonics” (www.munich-photonics.de) and the European Commission through the EU Project QAP and SCALA. W.W. acknowledges support by QCCC of the Elite Network of Bavaria and the Studienstiftung des deutschen Volkes.

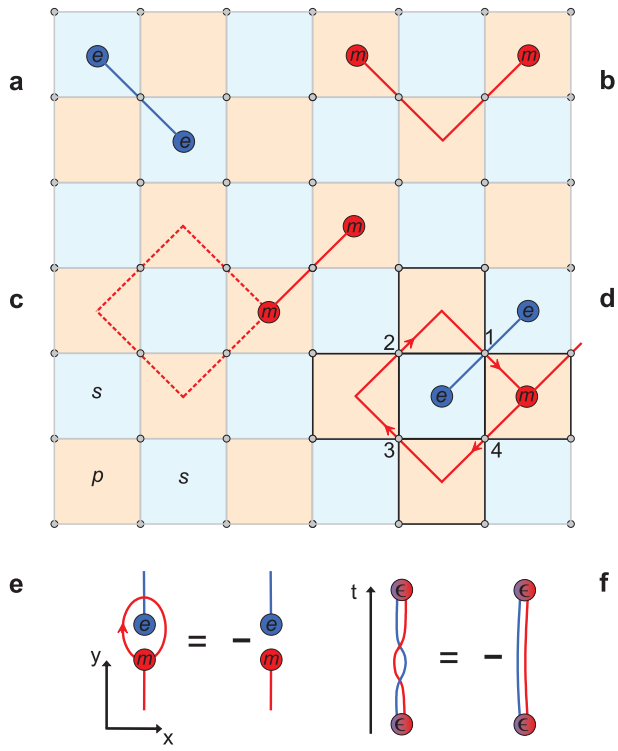
Competing Interests The authors declare that they have no competing financial interests.

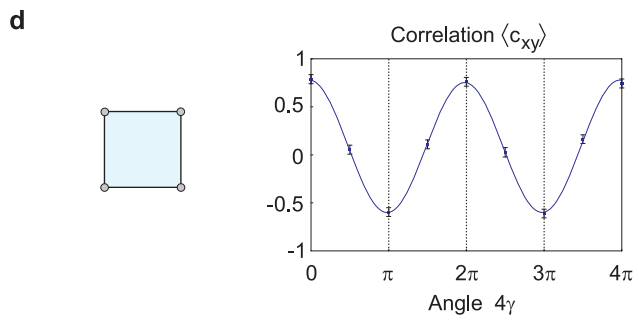
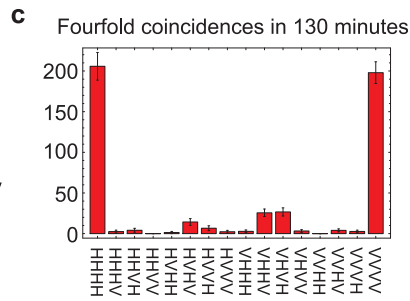
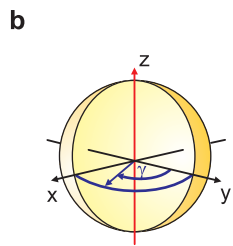
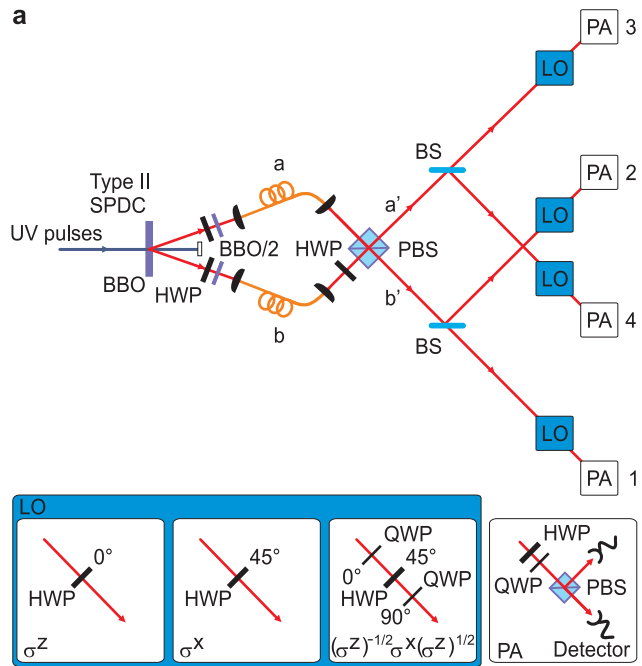
Correspondence Correspondence and requests for materials should be addressed to J.K.P. (email: j.k.pachos@leeds.ac.uk) and W.W. (email: witlef.wieczorek@mpq.mpg.de).

Supplementary Information The Supplementary Table S1 summarizes the experimental data taken for the anyonic measurements.

Supplementary Table S1. Measurement data for the creation and annihilation of anyons. Displayed are the obtained experimental values for the phase and fidelity of anyonic vacuum and anyonic populated states, with and without application of the loop operator $C_m = \sigma_1^x \sigma_2^x \sigma_3^x \sigma_4^x$. For anyonic vacuum states we expect a phase of 0, whereas for anyonic states a phase of π . A fidelity above 50% is sufficient to show genuine four-partite entanglement of the experimental states. All states satisfy this condition.

| | Phase ϕ | Fidelity F |
|---|------------------------------|--------------------|
| Vacuum state | | |
| $ \xi\rangle$ | $(0.02 \pm 0.01) \cdot \pi$ | $(74.5 \pm 2.2)\%$ |
| Creation of a single e-type anyon | | |
| $\sigma_1^z \xi\rangle$ | $(1.02 \pm 0.01) \cdot \pi$ | $(74.9 \pm 2.8)\%$ |
| $\sigma_2^z \xi\rangle$ | $(1.00 \pm 0.01) \cdot \pi$ | $(74.2 \pm 2.7)\%$ |
| $\sigma_3^z \xi\rangle$ | $(1.01 \pm 0.01) \cdot \pi$ | $(76.5 \pm 3.2)\%$ |
| $\sigma_4^z \xi\rangle$ | $(0.97 \pm 0.02) \cdot \pi$ | $(76.2 \pm 3.7)\%$ |
| String passing through the s plaquette | | |
| $\sigma_1^z \sigma_2^z \xi\rangle$ | $(0.02 \pm 0.01) \cdot \pi$ | $(77.4 \pm 2.8)\%$ |
| $\sigma_1^z \sigma_3^z \xi\rangle$ | $(0.01 \pm 0.01) \cdot \pi$ | $(77.3 \pm 2.5)\%$ |
| $\sigma_1^z \sigma_4^z \xi\rangle$ | $(-0.01 \pm 0.01) \cdot \pi$ | $(76.3 \pm 2.6)\%$ |
| String passing through the s plaquette populated with an anyon | | |
| $\sigma_2^z \sigma_4^z e\rangle$ | $(1.02 \pm 0.01) \cdot \pi$ | $(75.2 \pm 2.4)\%$ |
| $\sigma_3^z \sigma_4^z e\rangle$ | $(1.03 \pm 0.01) \cdot \pi$ | $(76.7 \pm 2.7)\%$ |
| $\sigma_1^z \sigma_4^z e\rangle$ | $(1.02 \pm 0.02) \cdot \pi$ | $(74.5 \pm 3.1)\%$ |
| Loop around an unpopulated s plaquette | | |
| $C_m \xi\rangle$ | $(-0.02 \pm 0.02) \cdot \pi$ | $(76.6 \pm 3.4)\%$ |
| Loop around a populated s plaquette followed by annihilation of the anyon | | |
| $(\sigma_4^z) C_m (\sigma_4^z) \xi\rangle$ | $(-0.01 \pm 0.01) \cdot \pi$ | $(76.8 \pm 2.8)\%$ |
| Interference procedure to reveal anyonic statistics | | |
| $(\sigma_1^z)^{1/2} C_m (\sigma_1^z)^{-1/2} \xi\rangle$ | $(1.03 \pm 0.01) \cdot \pi$ | $(76.1 \pm 3.0)\%$ |
| $(\sigma_2^z)^{1/2} C_m (\sigma_2^z)^{-1/2} \xi\rangle$ | $(0.99 \pm 0.01) \cdot \pi$ | $(73.5 \pm 3.6)\%$ |
| $(\sigma_3^z)^{1/2} C_m (\sigma_3^z)^{-1/2} \xi\rangle$ | $(1.01 \pm 0.01) \cdot \pi$ | $(75.2 \pm 3.0)\%$ |
| $(\sigma_4^z)^{1/2} C_m (\sigma_4^z)^{-1/2} \xi\rangle$ | $(1.00 \pm 0.01) \cdot \pi$ | $(75.8 \pm 2.5)\%$ |





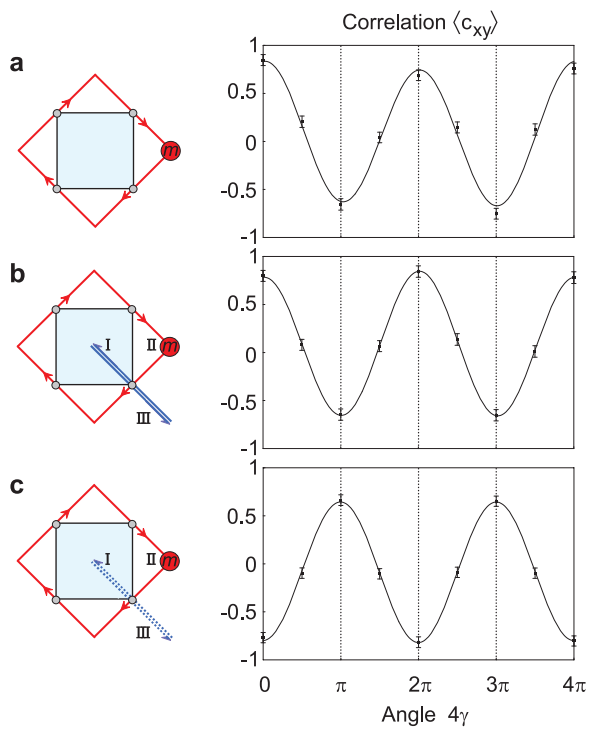
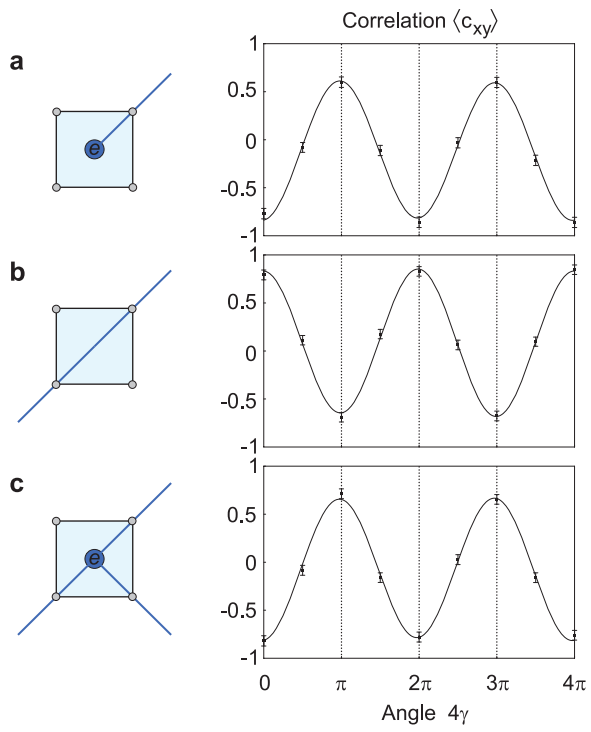


Figure 1 Toric code model and anyon braiding. The toric code model consists of alternating p - and s -plaquettes arranged in a chessboard fashion, where vertices represent physical qubits. Local operations acting on the qubits allow the creation and annihilation of anyons. **a**, Application of a σ^z Pauli rotation on a single qubit yields two e -type anyons placed at the neighbouring s plaquettes. **b**, Application of σ^x Pauli rotations on two neighbouring qubits would create four m -type anyons (on p plaquettes), where two m -type anyons are created on the same plaquette. These two anyons annihilate each other determined by the fusion rule $m \times m = 1$. Thus the two single strings are glued together with two anyons at its endpoints. **c**, When a part of a string forms a loop around an unpopulated plaquette it cancels (dashed). **d**, Here we restrict to the outlined system of one s plaquette and the four neighbouring p plaquettes. The anyonic vacuum state, $|\xi\rangle$, for this system is given by a four-qubit GHZ state between the qubits labelled 1 to 4 that constitute the s plaquette, while the remaining qubits are in a product state. Anyon e is produced by a σ^z Pauli rotation on qubit 1 (blue), $|e\rangle = \sigma_1^z |\xi\rangle$. This system can support the circulation of an m anyon around e . The transportation happens by successive σ_i^x rotations ($i = 1, 2, 3, 4$) at the qubits of the s plaquette (red). As the loop operator $C_m = \sigma_1^x \sigma_2^x \sigma_3^x \sigma_4^x$ anticommutes with σ_1^z and as $|\xi\rangle$ is invariant under the application of C_m , the final state is $-|e\rangle$. The minus sign demonstrates anyonic statistics between e and m . **e**, A pictorial representation of the braiding process that takes anyon m around e resulting in their relative statistical phase. **f**, The circulation of an m anyon around e is equivalent to a rotation of the composite particle $\epsilon = e \times m$ around itself as time evolves. Thus, the produced minus sign demonstrates the fermionic self-statistics of ϵ .

Figure 2 Diagram of the experimental set-up and experimental characterisation of the anyonic vacuum state. **a**, The anyonic vacuum and anyonic populated states are observed when a photon is registered in each spatial mode 1 to 4. The photons are created in a type II spontaneous parametric down conversion process (SPDC) in a β Barium Borate (BBO) crystal. They are coupled into single mode fibres and further processed by a half-wave plate (HWP), a polarising (PBS) and non-polarising beam splitters (BS). A detailed description can be found in the Methods section. All local operations (LO) performed on the anyonic vacuum state to demonstrate anyonic statistics are shown in the lower left corner. With a polarisation analysis (PA) the correlation measurements are performed. **b**, Shown is the Bloch sphere of one qubit depicting all relevant measurements: The measurement along the σ^z direction performed at each qubit from **c** is shown in red. The correlation function from **d** is measured along the x - y plane with an angle γ performed at each qubit (shown in blue). **c**, Correlation measurement of the anyonic vacuum state in the basis $\sigma_1^z \sigma_2^z \sigma_3^z \sigma_4^z$. We find the expected predominant populations P_{HHHH} and P_{VVVV} for a GHZ state and a correlation of $(0.908 \pm 0.047)\%$. **d**, Measured correlation function of the anyonic vacuum state with a pictorial representation of the s plaquette in this state. The displayed curve is given by a weighted least squares fit to a Fourier decomposition considering only even components up to order 4: $\sum_{k=0}^2 a_k \cos(2k \cdot \gamma) + b_k \sin(2k \cdot \gamma)$. Only these components can originate from physical states. The terms oscillating with 4γ can

be simplified to $\mathcal{V} \cos(4\gamma + \phi)$. The phase ϕ and visibility \mathcal{V} of the GHZ component are extracted from this decomposition and we find for the displayed curve $\phi = (0.02 \pm 0.01) \cdot \pi$ and $\mathcal{V} = (68.3 \pm 1.1)\%$.

Figure 3 Anyonic fusion rules. **a**, Generating an e -type anyon on an s plaquette by a σ^z -operation changes the state of the plaquette to $|e\rangle = |\text{GHZ}^\pi\rangle$. The phase ϕ of the state $|\text{GHZ}^\phi\rangle$ can be determined by analysing the correlation function $\langle c_{xy} \rangle = \mathcal{V} \cos(4\gamma + \phi)$, here with $\phi = 1.02\pi$. **b**, A second σ^z operation, now on qubit 3 removes the anyon from the plaquette and elongates the string connecting the pair of anyons. The observed phase of $\phi = 0.01\pi$ indicates the change back to the GHZ^0 state. **c**, A third σ^z on one of the remaining qubits of the plaquette creates another pair of anyons, connected with the string already traversing the plaquette. The phase of the plaquette state consequently changes to $\phi = 1.03\pi$.

Figure 4 Fractional statistics of anyons. Two possible evolutions, i.e., **a**, performing an s plaquette loop on an empty plaquette and **b**, first creating an anyon on the plaquette, performing the loop, and removing the anyon from the plaquette again give identical final states up to a global phase factor. This phase is equal to $+1$ for fermions and bosons, but different for anyons. **c**, We reveal the global phase by interfering the two above evolutions. This is achieved by first creating a superposition of empty and populated plaquette, performing the loop and removing the superposition again. A phase shift of $\phi = \pi$ proves the fractional statistics of anyons.